International Journal of Advanced Engineering, Management and Science (IJAEMS)
Peer-Reviewed Journal
ISSN: 2454-1311 | Vol-9, Issue-9; Sep, 2023
Journal Home Page: https://ijaems.com/
Article DOI: https://dx.doi.org/10.22161/ijaems.99.7

Experimental study of glass fiber concrete piles reinforced with GFRP bars and geogrid under concentric loads

EL Sayed A. El-kasaby[1], Mahmoud Awwad[2], Amir M. Mansour[3]

Civil Engineering Department Benha Faculty of Engineering, Benha University, Cairo, Egypt
[1]Prof. of soil mechanics and foundations. Email. Profkassaby@gmail.com
[2] Lecturer. Email. mahmoud.awad@bhit.bu.edu.eg
[3] Teaching Assistant. MSc Student. Email. amir.mohamed@bhit.bu.edu.eg

Received: 03 Aug 2023; Received in revised form: 05 Sep 2023; Accepted: 14 Sep 2023; Available online: 27 Sep 2023

Abstract— *In a variety of applications, glass fiber concrete has proven to be a successful substitute for supplying shear and flexural reinforcement for reinforced concrete. The mechanical properties of glass fiber concrete and steel reinforcement are different, hence the compression behavior of concrete piles reinforced with glass fiber concrete may be different from that of those reinforced with steel. However, the axial compression behavior of circular piles has not yet been established. This study assessed the concentric behavior of 12 end bearing piles with 1050 mm length and 150 mm diameter reinforced with varying amounts of glass fiber bristles (GFB), 0.75, 1.00, 1.25, and 1.50% of cement weight. The results are presented in this publication. 4 of them had no extra reinforcement (PG), 4 had glass fibre bars (GFRP) and spiral steel reinforcement (PGGB), and 4 had triaxial geogrid as reinforcement (PGG). All outcomes were contrasted with a pile that had steel reinforcement (PS). The findings demonstrated that theses composite piles increased the capacity of piles. The maximum load absorbed by the PG models under axial load was 3.54–21.43% less than the maximum load absorbed by PS. The PGGB specimen's maximum load was 0.00–30.03 % higher than the maximum load of PS specimen. The maximum load supported by the PGG specimens under axial load was, in some cases, 5.23–18.20% less than the maximum load supported by PS, while in another case, it was 17.51% more.*

Keywords*— *Glass fiber bristles, Glass fiber concrete piles, Geosynthetics, Composite pile, triaxial geogrid, and glass fiber bars.

I. INTRODUCTION

The advantages of glass fibre concrete (GC) include its high tensile strength, great durability, lightweight, and resilience to adverse environmental conditions. These characteristics make GC the appropriate substitute for traditional steel bars in concrete buildings that call for such properties. Numerous recent research has made examining the structural behavior of reinforced GC members their main goal. In the past two decades, a great deal of research has been done on the compression behaviour of GC-reinforced standard and high-strength concrete elements. Concrete columns with square cross section reinforced with GFRP bars and ties were studied [1-2]. Different types of fibers were used in concrete to improve its characteristics like steel, nano silica, polypropylene, carbon, and glass [3-5]. After that, a circular concrete column was examined experimentally and in field which reinforced with GFRP bars and ties with different testing parameters such as GFRP bars ratios, ties spacing, confinement reinforcement like hoops or spiral, and volumetric ratio [6-12].

High strength concrete (HSC) columns reinforced with GFRP bars and spirals have been tested to know its effect on column's resistance [13-15]. Behavior of different varieties of high-performance self-compacting concrete (HPSCC) has been studied for comparison with ordinary concrete, specimens were strengthened with steel rebars and various fibers [16]. After that, GFRP tubes filled with recycled and concrete material responded structurally when used to create composite piles [17]. Hollow concrete columns (HCCS) reinforced with GFRP bars and spirals were studied under different loading [18-19]. Composite piles have been tested which reinforced with different materials such as FRP bars, geosynthetics geogrids, and composite of two materials such as geogrid with a core of steel rod, and geogrid with a core of glass fiber reinforced polymers (GFRP) or carbon fiber reinforced polymers (CFRP) rod [20-21].

II. EXPERIMENTAL INVESTIGATION

2.1. Material

The concrete mix proportions utilized to cast the specimens are listed in Table 1. Both the nonfibrous and fibrous concrete had average compressive strengths of 15 and 20 MPa after 28 days, respectively. Steel bars in two distinct sizes, 8 mm plain mild rounded steel bars (R8) as longitudinal reinforcement and 6 mm plain mild rounded steel bars (R6) as transverse reinforcement were used to reinforce steel pile examples. The mechanical characteristics of the R8 and R6 steel bars, GFRP bars with size 8mm, Mesh of geogrid TX150 are given in Table 2,3,4 respectively. GFB are used to mix with concrete admixture with bristles length 12-16 mm and thickness of 0.01mm, Fig .1.

Fig. 1. Glass fibre bristles (GFB).

Table 1. The concrete mix proportions.

Material	Quantity (kg/m^3)
Cement	350
Fine aggregate	700
Coarse aggregate	1400
Water	175
Workability addition	0.4

Table 2. Mechanical properties of the steel bars.

Bar size	Diameter of the bar(mm)	Area of the bar (mm^2)	Yield tensile strength (MPa)	Strain (mm/mm)	Elastic modulus (GPa)
R8	8	50.29	240	0.0012	200
R6	6	28.29	240	0.0012	200

Table 3. Mechanical properties of the GFRP bars.

Bar size	Diameter of the bar(mm)	Area of the bar (mm^2)	Ultimate tensile strength (MPa)	Strain (mm/mm)	Tensile modulus (GPa)
#8	8	50.29	1100	0.0304	36

Table 4. Mechanical properties of geogrid.

Name	Thickness (mm)	Rib pitch (mm)		Ultimate tensile strength (MPa)	Tensile modulus (GPa)
		Longitudinal	Diagonal		
TX150	1.50	57	57	11.25	225

2.2. Design and processing of specimens

13 circular pile specimens with dimensions of 150 mm in diameter (D) and 1050 mm in height (L) and a ratio of 7 (L/D) were tested. The specimens were divided into three groups of four each, along with a typical steel-reinforced concrete pile control sample. Glass fibre was used to strengthen the 12 specimens in the three groups PG, PGGB, and PGG in varied amounts of GFB ,0.75, 1.00, 1.25, 1.25, 1.50% of cement weight. The first group of specimens lacks additional fortification. The second group's specimens (PGGB) were strengthened with four # 8 GFRP bars running longitudinally and R6 at 100mm pitch running transversely. These test models were created to determine

how the behavior of GC piles would change if the same amount of GFRP bars were directly substituted for the steel reinforcement. One roll of geogrid (TX150), which was constructed into the shape of a cylinder, was used to strengthen the specimens in the third group (PGG). These test specimens were created to determine how the behaviour of GC piles would change if the same amount of geogrid reinforcement were used directly in place of the steel reinforcement. Steel 4R8 longitudinal and R6 transverse bars are used to reinforce the control specimen. Table 5 displays the test matrix for the samples. The specimen's measurements and reinforcement setups are given in Fig. 2.

Table 5. Test matrix

Group	Pile code	Glass fiber %	Longitudinal reinforcement	Transverse reinforcement
Control (PS)	PS1	-	Steel 4R8	Steel R6@100mm pitch
PG	PG1	0.75	-	-
	PG3	1.00	-	-
	PG5	1.25	-	-
	PG7	1.50	-	-
PGGB	PGGB1	0.75	Glass 4#8	Steel R6@100mm pitch
	PGGB3	1.00		
	PGGB5	1.25		
	PGGB7	1.50		
PGG	PGG1	0.75	Roll of triaxial geogrid (TX150)	
	PGG3	1.00		
	PGG5	1.25		
	PGG7	1.50		

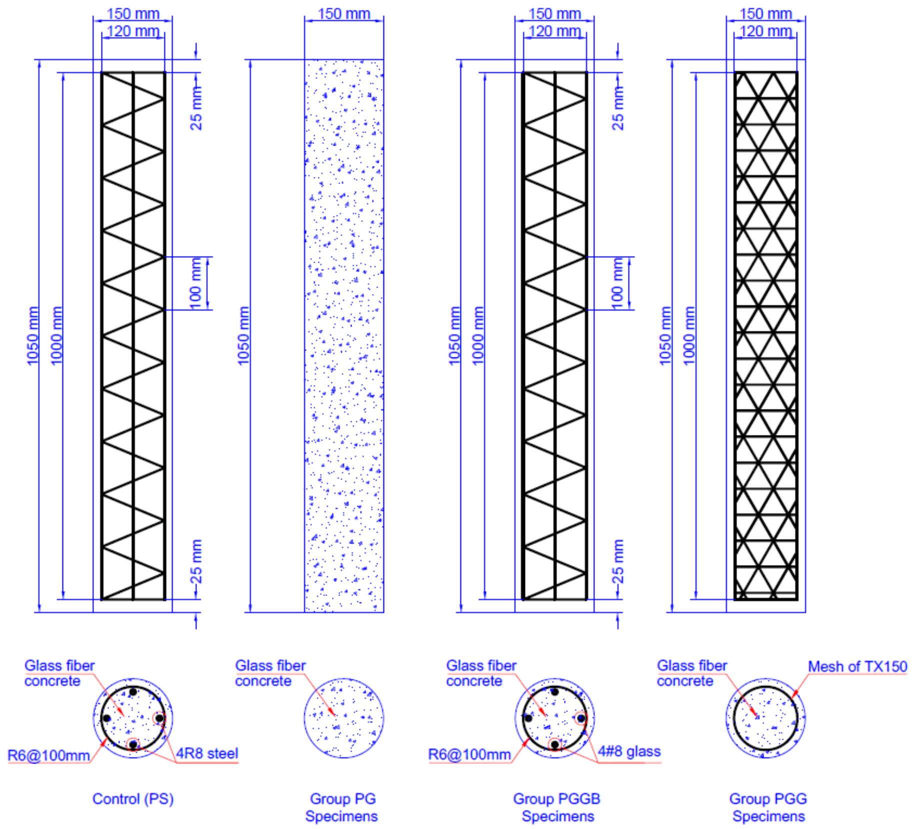

Fig.2. Geometry and reinforcement details of the tested specimens.

2.3. Creation and equipment of the test specimens

The specimens were cast using PVC pipes with an inner diameter of 150 mm and a height of 1050 mm as moulds. Additionally, a wooden frame was employed to support the PVC pipes upright and prevent any movement while the specimens were being cast. Based on the specimen's reinforcing configuration, geogrid reinforcement cages were put together. It was first cut into a rectangle of 1000 x 450 mm, and after that, it was rotated to take the form of a cylinder with a matching inner diameter of 120 mm, Fig. 3a. According to how each specimen's reinforcement was arranged, steel and GFRP reinforcement cages were put together. First, the GFRP and longitudinal steel bars were vertically aligned. After that, steel wire ties were used to combine the longitudinal bars with the reinforcing helices. To have the necessary pitch, the helices were modified. After that, the PVC moulds were filled with the finished reinforcement cages, Figs.3 b, c, d. The outer diameter of the steel and GFRP helices, which were manufactured, is 120 mm. The specimen's sides have a 15 mm concrete overlay. Additionally, 1000 mm-long longitudinal steel and GFRP bars were cut to maintain a consistent 25 mm concrete cover at the top and bottom of the specimen.

At the concrete laboratory of the civil engineering department, Benha University, Egypt, all the specimens were cast on the same day. The concrete mixture was directly put into the moulds created for PG, PGGB, and PGG specimens after being mixed with glass fibres in a concrete mixer. The ready mix was first added to the concrete mixer, after which the glass fibers were gradually added, uniformly distributed with a sieve, and stirred for approximately 10 minutes. The concrete mixture was then poured into the moulds created for PG, PGGB, and PGG specimens. In three steps, the specimens were vertically cast. Concrete was internally vibrated at every stage to eliminate air spaces and guarantee proper compaction. The specimens were retained in the moulds for the ensuing 28 days, during which time they were covered by wet burlap to cure, Fig. 3e.

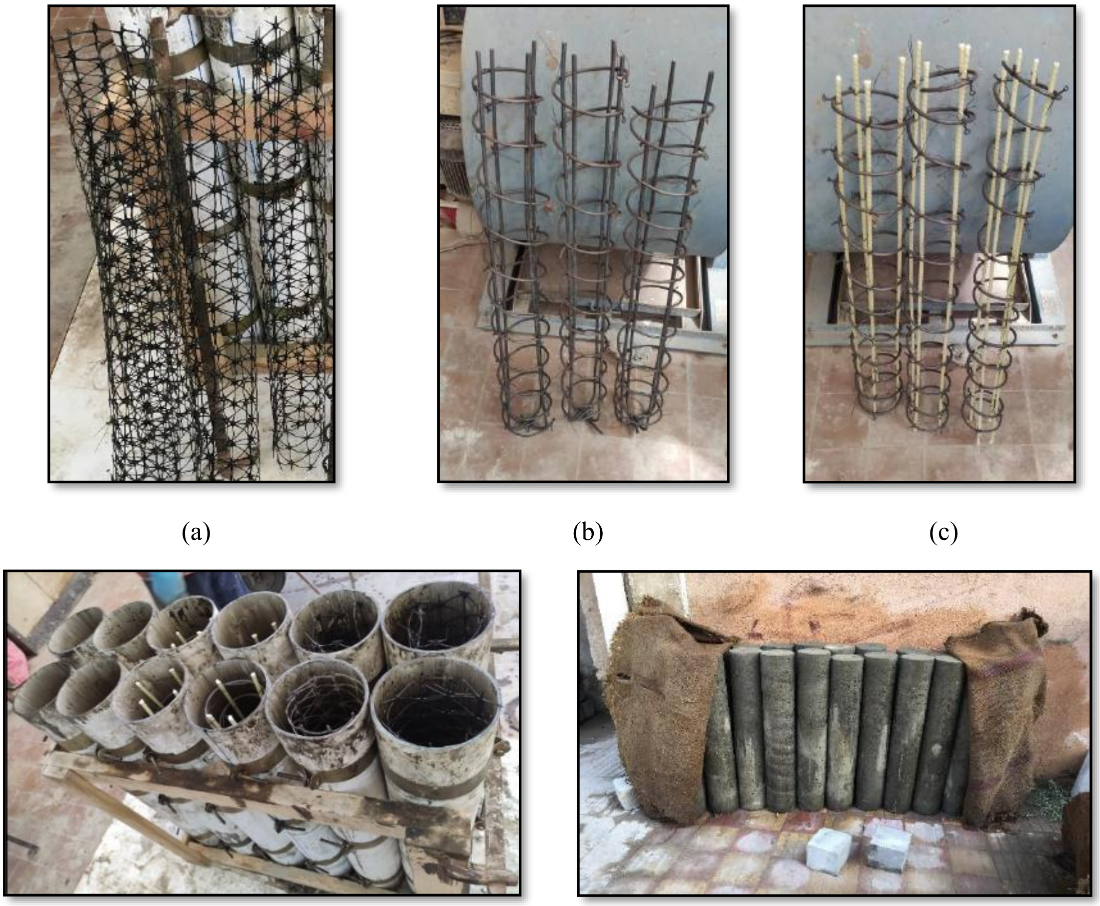

(a) (b) (c)

(d) (e)

Fig. 3. Fabrication of the tested specimens: (a) PGG specimens, (b) Ps specimen, (c) PGGB specimens, (d) completed formwork of the specimens and (e) specimen's curing.

2.4. Test configuration

The hydraulic Jac testing machine, which has a maximum compressive load capability of 1000 KN, was used to test all specimens. At the top and bottom of each specimen, axial loads were applied using two loading heads made at the Benha Faculty of Engineering. Steel ball joints and square steel plates made up each loading head. The ends of the specimens were shielded from bearing failure by square steel plates. The diameter of the tested specimens was smaller than the dimension of the square steel plates. The ends of the specimens were therefore not restrained by the square steel plates during the test as, Fig. 4.

Fig. 4. Setup testing of the pile specimens.

To detect the axial deformation in the column specimens during the test, one linear variable differential transducer (LVDT) was fixed vertically to the heads of the testing apparatus. At a pace of 5 kN/s, the specimens were loaded; force regulated. A data logger was connected to the LVDT to record data every 2 seconds. The internal load cell of the hydraulic Jac testing apparatus was used to record the applied axial load while the specimens were being tested.

III. RESULTS AND ANALYSIS

3.1. Failure mode

The type of reinforcement had a big impact on the test specimen's failure mechanisms. 13 piles investigated in this study showed three distinct causes of failure. Due to this specimen's lack of confinement, the failure modes of PG specimens were more abrupt, explosive, and brittle than those of any other specimens. The longitudinal steel bars of PS buckled which was followed by concrete crushing, Fig. 5a. The PG specimen's failure was a concrete smashing caused the unexpected failure, Fig. 5b. A combined compressive/shear failure of the longitudinal GFRP bars at their contact sites with the spirals, along with concrete crushing, caused all the PGGB specimens to fail, Fig. 5c. All the PGG specimens were destroyed by triaxial geogrid cutting and concrete crushing, Fig. 5d.

(a) (b)

(c) (d)

Fig. 5. Failure mode of tested specimens: (a) PS specimen, (b) PG specimens, (c) PGGB specimens, and (d) PGG specimens.

3.2. Effect of GFB %age

The results of Group 1 specimens can be used to determine the impact of the reinforcing % of GFB (PG1, PG3, PG5, and PG7). The 4 piles were made of the same concrete mixture but with varying amounts of GFB. The PG1, PG3, and PG5 had stress levels that were 5.72, 22.77, and 11.32 % higher than the PG7 respectively, Fig.6, Table 6. It is concluded that 1.00% is the ideal GFB %age (PG3). Despite this, maximum strain of PG1, PG3, and PG5 was around 44,20, and 15% less potent than PG7 respectively.

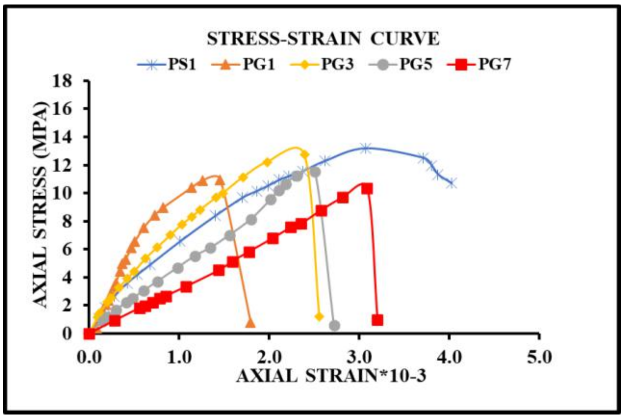

Fig. 6. Stress-strain behavior for GC piles.

Table 6. Stresses and strains for PG specimens.

Pile code	Max. stress (MPa)	Strain at max. stress (με)	Max strain(με)
PS1	13.19	3069	4022
PG1	10.96	1454	1793
PG3	12.72	2392	2560
PG5	11.54	2507	2720
PG7	10.36	3086	3200

3.3. Behavior of piles with GFRP bars and geogrid

Adding extra GFRP bars, spiral steel stirrups, and geogrid as the primary reinforcement for GC piles resulted in confinement for the piles, improved material behavior, increased both load capacity, strain, made the piles more ductile, and prevented brittle concrete failure.

It is possible to evaluate the impact of reinforcement type using the data of Group 2 specimens (PGGB1, PGGB3, PGGB5, and PGGB7). Four # 8 GFRP bars running longitudinally and four R6 at 100mm pitch running transversely, with varied GFB %ages, served as the principal reinforcement for the four piles. PGGB1, PGGB3, and PGGB5 had stress levels that were about 11.31, 31.93, and 14.97% higher than PGGB7 respectively, Fig.7, Table 7. The maximum strain of PGGB1 was roughly 35.86% lower than that of PGGB7, whereas PGGB3 and PGGB5 had maximum strains that were respectively 17.24 and 10.35% greater.

Results for Group 3 specimens provide information on the influence of reinforcement type (PGG1, PGG3, PGG5, and PGG7). The main reinforcement for the four piles was the same—a roll of TX150—but the GFB % varied. PGG1 experienced stress that was 6.72% less than PGG7, PGG3 and PGG5 experienced stress that was 16.42 and 8.06% greater than PGG7 respectively. PGG1's maximum strain was roughly 25.37% less than PGG7's, while PGG3's and PGG5's maximum strains were both about 16.42 and 4.48% greater respectively, Fig. 8, Table 8.

Table 7. Stresses and strains for PGGB specimens.

Pile code	Max. stress (MPa)	Strain at max. stress (με)	Max strain(με)
PS1	13.19	3069	4022
PGGB1	14.5	2025	2790

PGGB3	17.19	3185	5100
PGGB5	14.98	3500	4800
PGGB7	13.03	3800	4350

Table 8. Stresses and strains for PGG specimens.

Pile code	Max. stress (MPa)	Strain at max. stress (με)	Max strain(με)
PS1	13.19	3069	4022
PGG1	10.78	2000	2500
PGG3	15.5	3600	3900
PGG5	12.5	3100	3500
PGG7	11.57	3090	3350

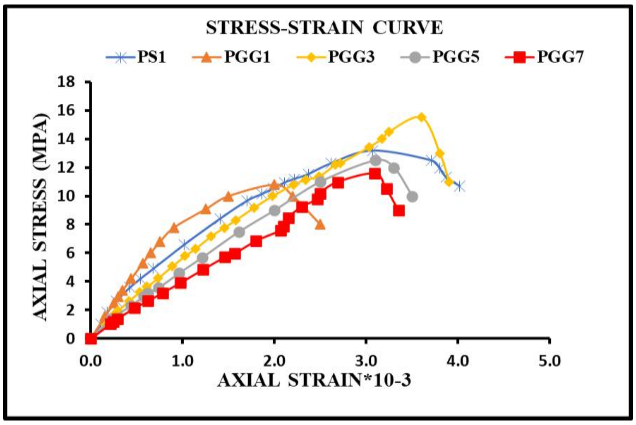

Fig. 8. Stress-strain behavior for PGG specimens.

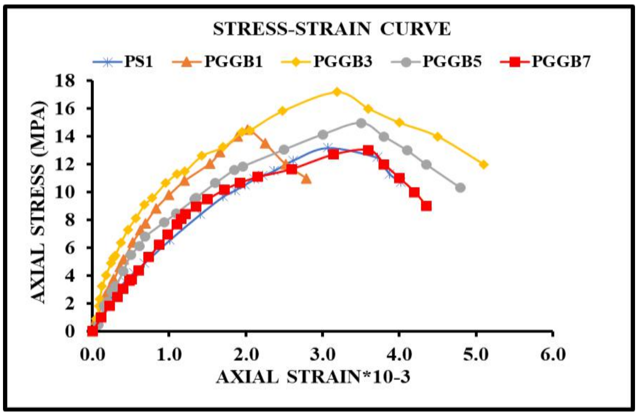

Fig. 7. Stress-strain behavior for PGGB specimens.

3.4. Behavior of GC piles with 1.00% GFB compared with steel pile.

The maximum stress and strain for PG3 were both roughly 3.54 and 36.36% smaller than those for PS1, respectively. When compared to the ductile failure of PS1, the failure was abrupt and brittle. Therefore, utilizing GFB as the primary reinforcement will roughly support the same load as steel reinforcement, but failure is the issue.

The maximum stress for PGG3 was approximately 17.51% higher than PS1's, whereas the maximum strain was approximately 3.04% lower. Triaxial geogrid confinement caused the failure to be ductile as steel reinforcement in PS1. Thus, employing the GFB with geogrid as reinforcement will carry more weight than using steel reinforcement while maintaining the same degree of elasticity, making this reinforcement more efficient.

The maximal stress and strain for PGGB3 were both about 30.29 and 26.79% more than that for PS1, respectively. The failure was more ductile than the steel reinforcement in PS1 because of the confinement of the steel stirrups and the high tensile strength of GFRP bars. It follows that employing GFB with GFRP bars as reinforcement will carry more weight than steel reinforcement and result in higher ductility, making this reinforcement the most efficient, Table 9 and Fig. 9.

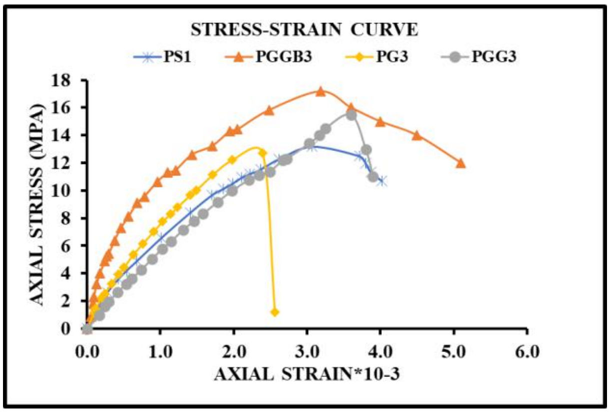

Fig. 9. Stress-strain behavior for 1.00% GFB specimens and steel.

Table 9. Stresses and strains for PGG specimens.

Pile code	Max. stress (MPa)	Strain at max. stress (με)	Max strain(με)
PS1	13.19	3069	4022
PG3	12.72	2392	2560
PGG3	15.5	3600	3900
PGGB3	17.19	3185	5100

IV. CONCLUSION

The outcomes of the experimental tests allow for the following summaries:

- Using glass fiber bars or geosynthetics geogrids as reinforcing materials enhanced the ultimate axial stress of the pile compared to the control pile specimen.
- In concrete piles, glass fiber bristles reinforcement made up 1.00% of the cement weight.
- Using glass fiber concrete as the main reinforcement under an axial load is less effective than using steel piles.
- In comparison to steel piles, using glass fiber concrete piles with glass fiber bars reinforcing provided the best vertical load resistance.
- The vertical loading capacity of using glass fiber concrete piles with geogrid reinforcement varied, sometimes being less than steel piles and other times being larger.
- The failure modes of specimens reinforced with glass fiber bristles were more abrupt, explosive, and brittle than those of any other specimens. All the other specimens were ductile due to the steel bars, glass fiber bars, and geogrid reinforcement.

ACKNOWLEDGMENTS

The Civil Engineering Department of Banha University and their support of this study effort through internal research are gratefully acknowledged by the authors. Also acknowledged are the technicians at the Civil Engineering Department's concrete laboratory for their assistance. I would like to express my sincere appreciation to the members of my advisory committee, for their support throughout my research program.

It was a great experience to work under the guidance of **Prof. EL Sayed Elkasaby**, whose valuable advice and encouragement were very important for the completion of this research.

REFERENCES

[1] De Luca A, Matta F, Nanni A. Behavior of full-scale glass fiber-reinforced polymer reinforced concrete columns under axial load. ACI Struct J. (2010);107(5).

[2] Tobbi H, Farghaly AS, Benmokrane B. Concrete columns reinforced longitudinally and transversally with glass fiber-reinforced polymer bars. ACI Struct J. (2012);109(4).

[3] Beigi MH, Berenjian J, Lotfi Omran O, Sadeghi Nik A, Nikbin IM. An experimental survey on combined effects of fibers and nanosilica on the mechanical, rheological, and durability properties of self-compacting concrete. Mater Des. (2013);50.

[4] Osorio LI, Paultre P, Eid R, Proulx J. Seismic behavior of synthetic fiber-reinforced circular columns. ACI Struct J. (2014);111(1).

[5] Saidani M, Saraireh D, Gerges M. Behaviour of different types of fibre reinforced concrete without admixture. Eng Struct. (2016);113.

[6] Mohamed HM, Afifi MZ, Benmokrane B. Performance evaluation of concrete columns reinforced longitudinally with FRP bars and confined with FRP hoops and spirals under axial load. Journal of Bridge Engineering. (2014);19(7).

[7] Afifi MZ, Mohamed HM, Benmokrane B. Axial capacity of circular concrete columns reinforced with GFRP bars and spirals. Journal of Composites for Construction. (2014);18(1).

[8] Afifi MZ, Mohamed HM, Benmokrane B. Theoretical stress-strain model for circular concrete columns confined by GFRP spirals and hoops. Eng Struct. (2015);102.

[9] Mousa S, Mohamed HM, Benmokrane B. Flexural strength and design analysis of circular reinforced concrete members with glass fiber-reinforced polymer bars and spirals. ACI Struct J. (2018);115(5).

[10] Maranan GB, Manalo AC, Benmokrane B, Karunasena W, Mendis P. Behavior of concentrically loaded geopolymer-concrete circular columns reinforced longitudinally and transversely with GFRP bars. Eng Struct. (2016);117.

[11] El-Gamal S, AlShareedah O. Behavior of axially loaded low strength concrete columns reinforced with GFRP bars and spirals. Eng Struct. (2020);216.

[12] Elchalakani M, Karrech A, Dong M, Ali MSM, Li GK, Yang B. Testing and modelling of geopolymer concrete members with fibreglass reinforcement. Proceedings of the Institution of Civil Engineers: Structures and Buildings. (2021);174(1).

[13] Hadhood A, Mohamed HM, Benmokrane B. Experimental study of circular high-strength concrete columns reinforced with GFRP bars and spirals under concentric and eccentric loading. Journal of Composites for Construction. (2017);21(2).

[14] Hadi MNS, Hasan HA, Sheikh MN. Experimental investigation of circular high-strength concrete columns reinforced with glass fiber-reinforced polymer bars and helices under different loading conditions. Journal of Composites for Construction. (2017);21(4).

[15] Hasan HA, Sheikh MN, Hadi MNS. Performance evaluation of high strength concrete and steel fibre high strength concrete columns reinforced with GFRP bars and helices. Constr Build Mater. (2017);134.

[16] Ding Y, Li D, Zhang Y, Azevedo C. Experimental investigation on the composite effect of steel rebars and macro fibers on the impact behavior of high performance self-compacting concrete. Constr Build Mater. (2017);136.

[17] Farhangi V, Karakouzian M. Effect of fiber reinforced polymer tubes filled with recycled materials and concrete on structural capacity of pile foundations. Applied Sciences (Switzerland). (2020);10(5).

[18] Alajarmeh O, Manalo A, Benmokrane B, Ferdous W, Mohammed A, Abousnina R, et al. Behavior of circular concrete columns reinforced with hollow composite sections and GFRP bars. Marine Structures. (2020);72.

[19] Al Ajarmeh OS, Manalo AC, Benmokrane B, Karunasena W, Ferdous W, Mendis P. A new design-oriented model of glass

fiber-reinforced polymer-reinforced hollow concrete columns. ACI Struct J. (2020);117(2).
[20] El-Kasaby ESA, Roshdy M, Awwad M, I. Badawi M. Behavior of composite piles reinforced by geosynthetics. International Journal of Advanced Engineering, Management and Science. (2023);9(4).
[21] El-Kasaby ES, Awwad M, Roshdy M, BADAWI M. Behavior of piles reinforced by geosynthetics under lateral load. MSA Engineering Journal. (2023);2(2).

